

A Census of Sun's Ancestors and their Contributions to the Solar System Chemical Composition

F. Fiore ^{*1}, F. Matteucci ^{1,2,3}, E. Spitoni ², M. Molero ^{4,2}, P. Salucci ^{5,3}, D. Romano ⁶ and A. Vasini ^{1,2}

¹ Dipartimento di Fisica, Sezione di Astronomia, Università di Trieste, Via G. B. Tiepolo 11, I-34143 Trieste, Italy

² I.N.A.F. Osservatorio Astronomico di Trieste, via G.B. Tiepolo 11, 34131, Trieste, Italy

³ I.N.F.N. Sezione di Trieste, via Valerio 2, 34134 Trieste, Italy

⁴ Institut für Kernphysik, Technische Universität Darmstadt, Schlossgartenstr. 2, Darmstadt 64289, Germany

⁵ SISSA-International School for Advanced Studies, Via Bonomea 265, 34136 Trieste, Italy

⁶ INAF, Osservatorio di Astrofisica e Scienza dello Spazio, Via Gobetti 93/3, I-40129 Bologna, Italy

Received xxxx / Accepted xxxx

ABSTRACT

In this work we compute the rates and numbers of different types of stars and phenomena (supernovae, novae, white dwarfs, merging neutron stars, black holes) that contributed to the chemical composition of the Solar System. During the Big Bang only light elements formed, while all the heavy ones, from carbon to uranium and beyond, were created inside stars. Stars die and restore the newly formed elements into the interstellar gas. This process is called "chemical evolution". In particular, we analyse the death rates of stars of all masses, dying either quiescently or explosively. These rates and total star numbers are computed in the context of a revised version of the two-infall model for the chemical evolution of the Milky Way, which reproduces fairly well the observed abundance patterns of several chemical species, as well as the global solar metallicity. We compute also the total number of stars ever born and still alive as well as the number of stars born up to the formation of the Solar System and with a mass and metallicity like the Sun. This latter number will account for all the possible existing Solar Systems which can host life in the solar vicinity. We conclude that, among all the stars (from 0.8 to 100 M_{\odot}) born and died from the beginning up to the Solar System formation epoch, which contributed to its chemical composition, 93.00% are represented by stars dying as single white dwarfs (without interacting significantly with a companion star) and originating in the mass range 0.8-8 M_{\odot} , while 5.24% are neutron stars and 0.73% are black holes, both originating from supernovae core-collapse ($M > 8 M_{\odot}$); 0.64% are Type Ia supernovae and 0.40% are nova systems, both originating from the same mass range as the white dwarfs. The number of stars similar to the Sun born from the beginning up to the Solar System formation, with metallicity in the range $12 + \log(\text{Fe}/\text{H}) = 7.50 \pm 0.04$ dex is $3.1732 \cdot 10^7$, and in particular our Sun is the $2.6092 \cdot 10^7$ -th star of this kind, born in the solar vicinity.

Key words. Galaxy: disk – Galaxy: abundances – Galaxy: formation – Galaxy: evolution – ISM: abundances

1. Introduction

Stars are born, live and die. During their lives they produce new chemical elements starting from H and He, in particular they form all the elements from ^{12}C to Uranium and beyond. They eject newly formed elements, both by stellar winds and through supernovae (SNe) explosions, thus increasing their abundance in the interstellar medium (ISM). This process is known as galactic chemical evolution and it is responsible for the chemical composition of the Solar System, that was born 4.6 Gyr ago (e.g., [Bouvier & Wadhwa 2010](#)). In order to study chemical evolution we need to build detailed models including several physical ingredients, such as star formation rate, initial mass function, stellar nucleosynthesis and gas flows.

In this paper we will focus on the Milky Way and in particular on the chemical evolution of the solar neighbourhood. Our main goal is to compute how many stars of different masses have contributed to build the chemical composition observed in the Solar System. In particular, we will analyse the contribution of low and intermediate mass stars dying as white dwarfs (WDs), SNe core-collapse (CC-SNe), and merging neutron stars (MNS). Moreover, we will compute the number of black holes

that have been created until the birth of the Solar System. To do that we adopt a detailed chemical evolution model which follows the evolution of several chemical species, for a total of 43 elements from H to Pb. The adopted model derives from the two-infall model originally developed by [Chiappini et al. \(1997\)](#) (see also [Matteucci et al. 2014](#); [Romano et al. 2019](#)). Here, we use the revised version of [Palla et al. \(2020\)](#) (see [Spitoni et al. 2019, 2020, 2021](#); [Molero et al. 2023](#)), focusing our study into the solar vicinity only.

The paper is organized as follows: in Section 2, we present the adopted chemical evolution model; in particular, we will describe the prescriptions we assumed for the initial mass function, star formation rate, stellar yields and gas flows. In Section 3, we will analyse the model results for each type of star and we will take a look at the evolution of α -elements relative to Fe. The plot of the ratio between α -elements ($\alpha = \text{O, Mg, Si, Ca}$) and Fe versus Fe can be used as a cosmic clock, thanks to the different timescales of production of α s and Fe (time-delay model, [Tinsley 1979](#); [Matteucci 2012](#)), and gives information on the past star formation history of the Galaxy. In Section 4 we will provide the rates and numbers of supernovae, white dwarfs, novae, merging neutron stars, and black holes occurred in the solar neighbourhood region until the formation of the Solar System. In Section

* email to: FRANCESCA.FIORE2@studenti.units.it

5, we will show the results obtained for the number of stars born roughly 4.6 ± 0.1 Gyr ago with the characteristics of the Sun: this is to have an idea of how many planetary systems similar to ours might have formed. Finally, in Section 6, we will provide the numbers of all stars and draw some conclusions.

2. Chemical Evolution Model: the Two-Infall Model

In order to discuss how different types of stars contribute to the chemical composition of the Solar System it is important to describe the original two-infall model (Chiappini et al. 1997), and the revised version by Palla et al. (2020) (see also Spitoni et al. 2019, 2021, 2024) that we will use in this paper. The two-infall model suggests that the Milky Way has formed in two main gas infall events. According to the original model, the first event should have formed the Galactic halo and the thick disk, while the second infall event should have formed the thin disk.

The *delayed* two-infall model adopted here is a variation of the classical two-infall model of Chiappini et al. (1997) developed to fit the dichotomy in the α -element abundances observed in the solar vicinity (Gratton et al. 1996; Fuhrmann 1998; Hayden et al. 2014; Recio-Blanco et al. 2014, 2023; Mikolaitis et al. 2017) as well as at different Galactocentric distances (e.g., Hayden et al. 2015). The model assumes that the first, primordial, gas infall event formed the thick disk whereas the second infall event, delayed by ~ 3 Gyr, formed the thin disk. It must be noted, that the two-infall model adopted here does not aim at distinguishing the thick and thin disk populations geometrically or kinematically (see Kawata & Chiappini 2016). The first gas infall event lasts about $\tau_1 \simeq 1$ Gyr, while for the second event an *inside-out* scenario (see e.g., Matteucci & Francois 1989; Romano et al. 2000; Chiappini et al. 2001) of Galaxy formation is assumed. Namely, the timescale of formation by gas infall of the various regions of the thin disk increases with Galactocentric distance. It should be noticed that the two main episodes described by the two-infall model are sequential in time but they are completely independent. In the original model of Chiappini et al. (1997), it was assumed a threshold gas density for star formation which naturally produces a gap in the star formation between the end of the thick disk phase and the beginning of the thin disk, and therefore a dichotomy in the $[\alpha/\text{Fe}]$ vs. $[\text{Fe}/\text{H}]$. However, even without the assumption of a gas threshold, the situation of the two-infall episodes creates a dichotomy by itself, although less pronounced, but enough to reproduce the data (see Spitoni et al. 2019).

2.1. The basic equations of chemical evolution

The basic equations which describe the evolution in the solar vicinity of the fraction of gas mass in the form of a generic chemical element i , G_i , are:

$$\dot{G}_i(R, t) = -\psi(R, t)X_i(R, t) + \dot{G}_{i,\text{infall}}(R, t) + \dot{E}_i(R, t), \quad (1)$$

where X_i is the abundance by mass of the analysed element, $\psi(t)$ is the star formation (SF), $\dot{G}_{i,\text{infall}}(R, t)$ is the gas infall rate and $\dot{E}_i(R, t)$ is the rate of variation of the returned mass in the form of the chemical species i , both newly formed and restored unprocessed. This last term contains all the stellar nucleosynthesis and stellar lifetimes.

2.2. Star Formation Rate

The quantity we are interested in here is the so-called stellar birthrate function, namely the number of stars with mass dm

which are formed in the time interval dt . It is factorized as the product of the SF, depending only on the time t , with the IMF, here assumed to be independent of time and being only a function of the mass m .

For the SF rate (SFR), here we adopt as parametrization the common Schmidt-Kennicutt law (Schmidt 1959; Kennicutt 1998), according to the SFR is proportional to the k th power of the surface gas density. The SFR can be written as:

$$\psi(t) \propto \nu \sigma_{\text{gas}}^k(t), \quad (2)$$

where ν is the efficiency of star formation, namely the SFR per unit mass of gas, and it is expressed in Gyr^{-1} . For the halo-thick disk phase $\nu = 2 \text{ Gyr}^{-1}$, whereas for the thin disk ν is a function of the Galactocentric distance R_{GC} , with $\nu(R_{GC}=8 \text{ kpc}) \simeq 1 \text{ Gyr}^{-1}$, as in Molero et al. (2023) and Palla et al. (2020). It is important to highlight that gas temperature, viscosity and magnetic fields are ignored in this empirical law even if they are quite important parameters. Nevertheless, ignoring these parameters is a common choice for the SFR in most of galaxy evolution models.

In the scenario described by the original two-infall model there was supposed to be a gas threshold in the star formation. This created a stop in the star formation process between the formation of the thick and the thin disk. Here, we relax the assumption of a threshold in the gas density and the gap in the star formation is *naturally* created between the formation of the two disks, since, because of the longer delay between the two infall episodes, the SFR becomes so small that a negligible number of stars is born in that time interval.

In this context, we can make an additional distinction in the phases described by the two-infall model based on the stars that were present and dominating at each time. During the thick disk formation, the most important contribution was from core-collapse supernovae (CC-SNe) which are identified by Type II, Ib, and Ic ones, while Type Ia supernovae started giving a substantial contribution only after a time delay (see Matteucci 2021). This important difference impacts significantly on the production of chemical elements and Galaxy composition and it is known as the *time-delay model* (Tinsley 1979; Matteucci 2012, 2021).

2.3. Initial Mass Function

The second ingredient in the stellar birthrate function is the initial mass function (IMF) which gives the distribution of stellar masses at birth and it is commonly parameterised as a power law. As to measure the IMF it is necessary to count the stars as functions of their magnitude, nowadays we can only do that for the solar region of the Milky Way. We use as IMF the one proposed by Kroupa et al. (1993), which in chemical evolution is often the one which provides the best agreement with observations (see Romano et al. 2005 for a discussion). It is a three slopes IMF, with the following expression:

$$\phi(m) = C \begin{cases} m^{-(1+0.3)} & \text{if } m \leq 0.5M_{\odot} \\ m^{-(1+1.2)} & \text{if } 0.5 < m/M_{\odot} < 1.0 \\ m^{-(1+1.7)} & \text{if } m > 1.0M_{\odot}, \end{cases} \quad (3)$$

with C being the normalization constant derived by imposing that:

$$1 = \int_{0.1}^{100} m\phi(m) dm, \quad (4)$$

where $\phi(m)$ is the IMF in number.

2.4. Gas Flows

The gas flows are of fundamental importance for studying the chemical composition of the Galaxy, since they are required to explain several features, such as the abundance gradients along the disks (Grisoni et al. 2018; Palla et al. 2020). In the case of infall gas flows, the gas is often assumed to have a primordial composition, namely with zero metal content. Since the gas is enriched only in light elements such as H, He and a small part of Li and Be, the effect of the infall is that of diluting the metal content inside the Galaxy. In this work, different gas flows than the infall one (such as Galactic winds and/or Galactic fountains) are not included. In particular, Galactic fountains, which can occur in disk galaxies, have been proven not to impact in a significant manner the chemical evolution of the disk (see Melioli et al. 2009).

In the context of the revised two-infall model adopted here, the accretion term is computed as:

$$\dot{G}_{i,inf}(R, t) = AX_{i,inf}e^{-\frac{t}{\tau_1}} + \theta(t - t_{max})BX_{i,inf}e^{-\frac{t-t_{max}}{\tau_2}}, \quad (5)$$

where $X_{i,inf}$ is the composition of the infalling gas, here assumed to be primordial for both the infall events. $\tau_1=1$ and $\tau_2=7$ Gyr are the infall timescales for the first and the second accretion event, respectively, and $t_{max} \simeq 3.25$ Gyr is the time for the maximum infall on the disk and it corresponds to the start of the second infall episode. The parameters A and B are fixed to reproduce the surface mass density of the MW disc at the present time in the solar neighbourhood. Particularly, A reproduces the present time thick disk total surface mass density ($12 M_{\odot} \text{ pc}^{-2}$), while B does the same for the present time thin disk total surface mass density ($54 M_{\odot} \text{ pc}^{-2}$), at the solar ring (Molero et al. 2023). We remind that the θ function is the Heavyside step function.

2.5. Element production and chemical yields

It is worth reminding that different elements are produced in different stars. In particular:

- Brown dwarfs with mass $< 0.1 M_{\odot}$ do not ignite H, so they do not contribute to chemical enrichment of the ISM, but they affect the chemical evolution by locking up gas;
- Very small stars in the mass range $0.1 M_{\odot} - 0.8 M_{\odot}$ burn only H. They die as He-white dwarfs;
- Low and intermediate mass stars (LIMs) in the mass range $0.8 M_{\odot} - 8.0 M_{\odot}$, they contribute to the chemical enrichment through post-MS mass loss and the final ejection of a planetary nebula. They produce mainly ^4He , ^{12}C and ^{14}N plus some CNO isotopes and heavy ($A > 90$) s-process elements;
- White dwarfs in binary systems can give rise to Type Ia SNe or novae. Type Ia SNe are responsible for producing the bulk of Fe ($\simeq 0.60 M_{\odot}$ per event) and enrich the medium with tracers of elements from C to Si. They also contribute to other elements, such as C, Ne, Ca and Mg, but in a much less amount compared to CC-SNe. Novae can be important producers of CNO isotopes and perhaps ^7Li ;
- Massive stars from 8 to $10 M_{\odot}$ burn O explosively (e-capture supernovae). They produce mainly He, C and O. They leave neutron stars as remnants;
- Massive stars in the mass range $10 M_{\odot} - M_{WR}$ end their life as Type II SNe and explode by core-collapse. The explosion leads to the formation of a neutron star or a black hole, depending on the amount of mass loss during the star life and ejected material which falls back on the contracting

core. M_{WR} is the minimum mass for the formation of a Wolf-Rayet star. Its value depends on the stellar mass loss which in turn depends on the progenitor characteristics in term of initial mass and metallicity. For a solar chemical composition, $M_{WR} \simeq 25 M_{\odot}$. Stars with masses above M_{WR} end up as Type Ib/c and explode also by core-collapse. They are linked to the long Gamma Ray Bursts (LGRBs) and can be particularly energetic so to be know as hypernovae (HNe, Paczyński 1998). Massive stars are responsible for the production of most of *alpha*-elements (such as O, Ne, Mg, Si, S, Ca), some Fe-peak elements, light ($A < 90$) s-process elements (especially if stellar rotation is included) and may contribute also to r-process nucleosynthesis (if strong magnetic field and fast rotation are included).

- Merging of compact object and in particular neutron stars binary systems are powerful sources of r-process material.

The stellar yields that we adopt for stars of all masses, Type Ia SNe and merging neutron stars are similar to those adopted in Romano et al. (2010) and Molero et al. (2023). In particular, we adopt the yields of massive stars of Kobayashi et al. (2006) and the Geneva group (Meynet & Maeder 2002; Hirschi 2005, 2007; Ekström et al. 2008) yields for what concerns the CNO elements. For low and intermediate mass stars yields we assume those of Karakas (2010); for Type Ia SNe, those of Iwamoto et al. (1999) and for neutron capture elements those adopted by Molero et al. (2023) for merging neutron stars as well as for massive stars dying as magneto-rotational supernovae (MR-SNe).

3. Results: SFR and abundances

As it has been explained in Section 1, it is important to understand how many stars are in the Milky Way for each type. However, before presenting the obtained model results it is necessary to introduce the *time-delay model* and how it affects the abundance patterns in the typical $[\text{X}/\text{Fe}]^1$ vs. $[\text{Fe}/\text{H}]$ diagrams. Since our goal is to compute how many stars of different kind contributed to the chemical composition of the Solar System, results of the chemical evolution model will be presented until the formation of the Solar System, commonly assumed to be about 9.2 Gyr after the Big Bang, namely 4.6 Gyr ago.

Before presenting the analysis of the abundance patterns, it is important to compare the evolution of the SFR predicted by our model at $R_{GC}=8$ kpc to present-day observations in the solar vicinity. The SF rate, expressed in units of $M_{\odot} \text{ pc}^{-2} \text{ Gyr}^{-1}$, is shown in Figure 1. The gap between the two different disk phases is clearly visible and the present-day value predicted by our model appears to be in nice agreement with the measured range in the solar neighborhood suggested by Prantzos et al. (2018).

To compute how many solar masses of stars have been formed until the moment of the formation of the Solar System, we computed the integral of the SFR in the time interval 0.0 - 9.2 Gyr, as:

$$\int_{0.0}^{9.2 \text{ Gyr}} \psi(t) dt = 51 M_{\odot} \text{ pc}^{-2}. \quad (6)$$

This value, once multiplied by the area of the solar annular ring 2 kpc wide ($\sim 10^8 \text{ pc}^2$), gives the total mass of stars ever formed, equal to $5.1 \times 10^9 M_{\odot}$. We stress that this quantity takes into

¹ we remind that the notation $[\text{X}/\text{Y}]$ has the meaning $[\text{X}/\text{Y}] = \log(\text{X}/\text{Y}) - \log(\text{X}/\text{Y})_{\odot}$ with X (Y) being the abundance by number of the element X (Y).

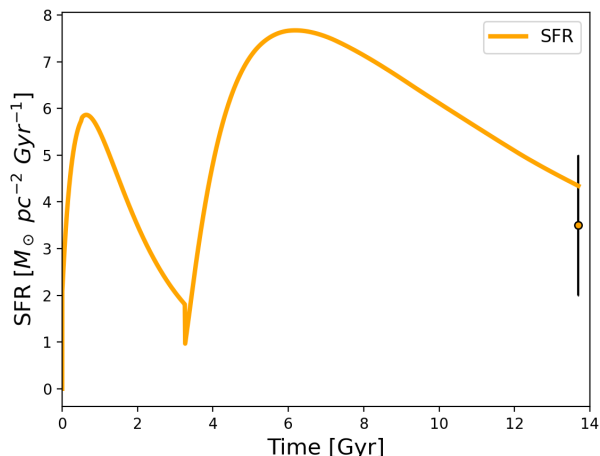


Fig. 1. SFR time evolution predicted by the two-infall model for the solar vicinity. Observed present day value is from Prantzos et al. (2018).

account also the contribution from the stellar remnants (namely white dwarfs, neutron stars and black holes).

For what concerns the total metallicity in the ISM 4.6 Gyr ago, we predict $Z_{\odot}=0.0130$, in excellent agreement with the solar metallicity by Asplund et al. (2009, $Z_{\odot}=0.0134$), and the Fe abundance is $12 + \log(\text{Fe}/\text{H})_{\odot}=7.48$, again in excellent agreement with the observed abundance.

3.1. The time-Delay Model

To explain the abundance pattern of α -elements in the common $[\alpha/\text{Fe}]$ vs $[\text{Fe}/\text{H}]$ diagrams, it is necessary to first introduce the time-delay model. The *time-delay model* (Tinsley 1979; Matteucci & Greggio 1986) explains the observed abundance patterns in terms of different chemical elements produced by different types of stars on different time-scales. In the case of α -elements, they are mostly produced by CC-SNe on short timescales (typically below 30 Myr). CC-SNe are producing also Fe, however the bulk of it is produced by Type Ia SNe. Since, as indicated above, Type Ia SNe are the results of exploding white dwarfs in binary systems, they live more than 30 Myr and up to 10 Gyr, and therefore the Fe by Type Ia SNe is produced on longer time-scales. As a consequence, when it comes to the α -elements abundance trends, we usually observe high $[\alpha/\text{Fe}]$ ratios at low $[\text{Fe}/\text{H}]$ values, where the production of both α -elements and Fe is due only to CC-SNe, and lower $[\alpha/\text{Fe}]$ ratios at high $[\text{Fe}/\text{H}]$ because of the late contribution from Type Ia SNe. Since as time pass by more and more generations of stars succeed and enrich the ISM with heavy elements, the $[\text{Fe}/\text{H}]$ axis can be seen as a time axis because the Fe abundance increases in time. As a consequence, the knee which is observed in the $[\alpha/\text{Fe}]$ vs. $[\text{Fe}/\text{H}]$ trends at $[\text{Fe}/\text{H}] \sim -1.0$ dex corresponds to the time at which Type Ia SNe become important as Fe producers. This $[\text{Fe}/\text{H}]$ value changes with different SFRs and therefore will be different in different environments.

3.2. Analysis of the $[\alpha/\text{Fe}]$ vs $[\text{Fe}/\text{H}]$ plot

In this section, we will present and analyse the $[\alpha/\text{Fe}]$ vs. $[\text{Fe}/\text{H}]$ abundance patterns of some α -elements, namely O, Mg, Si and Ca. Figure 2 shows the plots of $[\alpha/\text{Fe}]$ vs. $[\text{Fe}/\text{H}]$ ($\alpha = \text{O}, \text{Mg}, \text{Si}, \text{Ca}$) predicted by the model. The time-delay model (Tins-

ley 1979; Matteucci 2012) provides a satisfying explanation for these paths: the ratio of $[\alpha/\text{Fe}]$ at low metallicity is rather flat, although the slope on the nucleosynthesis of different α -elements because only CC-SNe produce α elements and some amount of Fe, so this part of the plot is representative only of the contribution to the $[\alpha/\text{Fe}]$ ratio from massive stars. At $[\text{Fe}/\text{H}] \geq -1.0$ dex, Type Ia SNe start giving their contribution in a substantial way, as it can be seen from the knee shown in the plots. This happens because, as it was already explained, Type Ia SNe are the main producers of Fe and they eject this element in the ISM on longer timescales. The loop shown by the curves in Figure 2, is due to the gap in the star formation occurring in between the two infall events. In fact, as explained in Spitoni et al. (2019), the second infall causes a dilution of the absolute abundances, producing an horizontal stripe in the $[\text{Fe}/\text{H}]$ at almost constant $[\alpha/\text{Fe}]$. Then, when the SF recovers, the $[\alpha/\text{Fe}]$ ratio rises and then decreases slowly because of the advent of Type Ia SNe. These loops can successfully explain the bimodality in $[\alpha/\text{Fe}]$ ratios (Spitoni et al. 2019, 2020).

Since the x-axis should be interpreted as a time axis, the $[\alpha/\text{Fe}]$ vs. $[\text{Fe}/\text{H}]$ relation can be used to extract the timescale for the formation of the thick and thin disks, knowing that thick disk stars have metallicity ≤ -0.6 dex. Originally, Matteucci & Greggio (1986) derived the timescale of the formation of the inner halo-thick disk to be around 1.0-1.5 Gyr. Subsequent studies dealing with detailed evolution of the thick disk have confirmed a timescale of ~ 1 Gyr for the formation of the thick disk (e.g. Micali et al. 2013; Grisoni et al. 2017). Here, we find the same timescale. It is worth noting that the timescale of formation of the thin disk at the solar ring is provided by the fit to the G-dwarf metallicity distribution and is 7 Gyr (e.g. Grisoni et al. 2017).

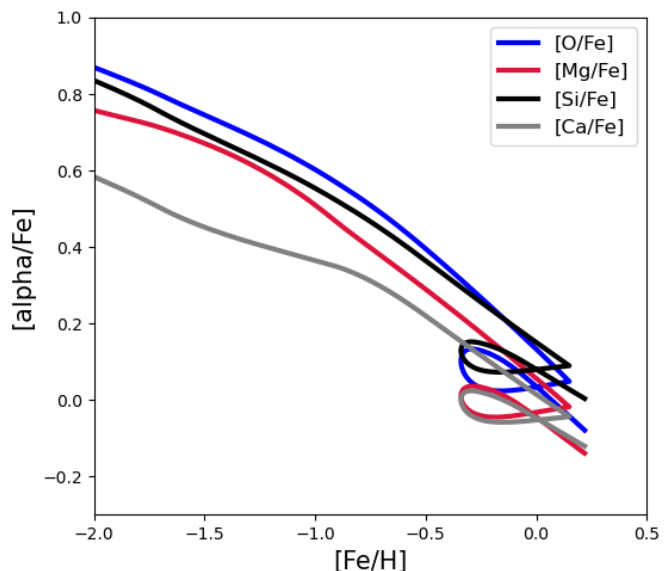


Fig. 2. $[\alpha/\text{Fe}]$ versus $[\text{Fe}/\text{H}]$ abundance ratios predicted by our fiducial chemical evolution model for different α -elements: oxygen (blue line), magnesium (red line), silicon (black line) and calcium (grey line), for the solar vicinity.

4. Results: Rates and Numbers of supernovae, white dwarfs, novae, merging neutron stars, and black holes

Since we reproduce quite well the solar metallicity and the abundance patterns in the solar vicinity, now we can proceed to compute in detail the rates and numbers of supernovae (Type Ia and core-collapse), white dwarfs, novae, neutron stars and black holes occurred until the formation of the Solar System.

Let us introduce now two areas in use in this paper. We define, unless otherwise stated, as solar vicinity the annular region 2 kpc wide centered in the Sun, whose area is approximately 10^8 pc². For the whole disc we assume an area of approximately 10^9 pc².

4.1. Type Ia Supernovae

To compute the number of Type Ia SNe exploded until the formation of the Solar System, we proceed just in the same way as for the total number of stars formed (see previous Section). In particular, we compute their rate as the fraction of white dwarfs in binary systems that have the necessary conditions to give rise to a Type Ia SN event. This allows us to compute the rate of Type Ia SNe as suggested by [Greggio \(2005\)](#):

$$(Rate)_{SNeIa}(t) = K_\alpha \int_{\tau_i}^{\min(t, \tau_x)} A(t-\tau) \psi(t-\tau) DTD(\tau) d\tau, \quad (7)$$

where τ is the total delay time, namely the nuclear stellar lifetime of the secondary component of the binary system plus a possible delay due to the gravitational time delay in the DD model. $A(t-\tau)$ is the fraction of binary systems which give rise to SNe Type Ia and we assume it constant in time. The DTD(t) is the Delay Time Distribution, describing the rate of explosion of Type Ia SNe for a single starburst. The DTD is normalised as:

$$\int_{\tau_i}^{\tau_x} DTD(\tau) d\tau = 1, \quad (8)$$

with τ_i being the lifetime of a $\sim 8 M_\odot$ star and τ_x the maximum time for the explosion of a Type Ia SN. Here, we adopt the DTD for the wide DD scenario as suggested by [Greggio \(2005\)](#), where a detailed description can be found (see also [Simonetti et al. 2019](#); [Molero et al. 2021](#)). Finally, K_α is a function of the IMF, namely

$$K_\alpha = \int_{0.1 M_\odot}^{100 M_\odot} \varphi(m) dm. \quad (9)$$

The predicted present-time Type Ia SN rate for the whole disk is:

$$(Rate)_{SNeIa} = 0.40 \cdot \text{events/century}. \quad (10)$$

It is important to notice that this result is compatible with observational data of 0.43 events/century ([Cappellaro & Turatto 1997](#); [Li et al. 2011](#)) which confirms the validity of the model.

We then compute the number of Type Ia SNe until the birth of the Solar System, in the solar vicinity. To do so, we integrate the rate from 0 Gyr to 9.2 Gyr, obtaining:

$$N_{SNeIa} = \int_0^{9.2 \text{ Gyr}} (Rate)_{SNeIa} dt = 2.87 \cdot 10^6. \quad (11)$$

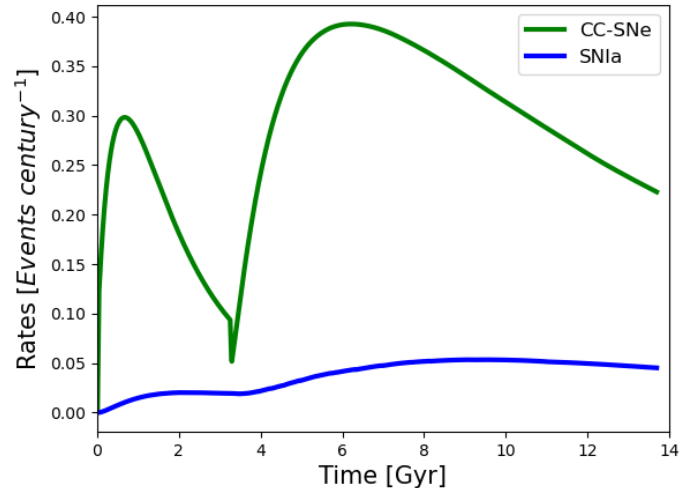


Fig. 3. Predicted rate of core-collapse (green line) compared to that of Type Ia supernovae (blue line) in the solar vicinity.

4.2. Core-Collapse Supernovae

We compute the fraction of massive stars that will die as a CC-SN by assuming that they originate from single massive stars or massive binaries. The rate of Type II supernovae is computed as:

$$(Rate)_{SNeII}(t) = \int_{8 M_\odot}^{M_{WR}} \psi(t-\tau_m) \varphi(m) dm, \quad (12)$$

where, as previously described, M_{WR} is the limiting mass for the formation of a Wolf-Rayet star. The rate of Type Ib/Ic SNe can be calculated as (see [Bissaldi et al. 2007](#)):

$$(Rate)_{SNeIb,c}(t) = (1-\gamma) \int_{M_{WR}}^{M_{max}} \psi(t-\tau_m) \varphi(m) dm + \gamma \int_{14.8 M_\odot}^{45 M_\odot} \psi(t-\tau_m) \varphi(m) dm, \quad (13)$$

where the parameter γ is chosen to reproduce the number of massive binary systems in the range $14.8 \div 45 M_\odot$ and this range of masses of stars is the one proposed by [Yoon et al. \(2010\)](#) to produce a SNeIb,c. The mass M_{max} is the maximum mass allowed by the IMF, equal to $100 M_\odot$.

Considering both SNeII and SNeIb,c, we obtain a total rate of CC-SNe of $(Rate)_{CCSNe} = 2.23$ events/century which is in agreement with the observational data of 1.93 events/century ([Cappellaro & Turatto 1997](#)). The total number of CC-SNe exploded until the formation of the Solar System, in the solar vicinity, is:

$$N_{CCSNe} = \int_0^{9.2 \text{ Gyr}} (Rate)_{CCSNe} dt = 26.47 \cdot 10^6. \quad (14)$$

In Figure 3 we can see the CC-SNe rate behaviour and appreciate the fact that, as expected, it follows the SFR path. In the same Figure we show the Type Ia SN rate as a function of time, in the solar vicinity. In Table 1, we finally summarised our results compared to observational data.

Table 1. Comparison between observational data relative to SN rates (Cappellaro & Turatto 1997) compared with model results. We can see that all theoretical values are consistent with observational data. In the first column there are the observed rates, in the second column the predicted ones and in the third column are the computed total numbers of SNe exploded from the beginning up to the formation of the Solar System.

	Observational Data (whole disc, present-day)	Rates (whole disc, present-day)	Numbers (solar vicinity, 9.2 Gyr of evolution)
SN Ia	0.43 <i>SNe/century</i>	0.45 <i>SNe/century</i>	2.87 million
CC-SNe	1.93 <i>SNe/century</i>	2.23 <i>SNe/century</i>	26.47 million

4.3. White Dwarfs and Novae

In Figure 4, we plot the rate of formation of white dwarfs, originating in the mass ranges $0.8-8 M_{\odot}$, from which we obtain the number of white dwarfs that formed until the moment of formation of the Solar System., in the solar vicinity. This is computed as:

$$N_{WD} = \int_0^{9.2 \text{ Gyr}} (Rate)_{WD} dt = 423.88 \cdot 10^6. \quad (15)$$

A nova outburst is caused by thermonuclear runaway on top of a white dwarf accreting H-rich matter from a close companion (a main sequence or a giant star) that overfills its Roche lobe. The system survives the explosion and the cycle is repeated some 10^4 times. There are various ways to compute the rate of novae in our Galaxy, such as using the known novae to extrapolate for those too far to be seen or else observing novae in another galaxy and extrapolate their rate in the Milky Way by assuming that every nova from the other galaxy can be seen.

We compute the nova rate by assuming that it is a fraction of the white dwarf rate. To do so, it is appropriate to define a parameter, $\alpha_{nova} < 1$, that represents the fraction of white dwarfs that will form novae, and it is tuned to reproduce the present time nova rate in the Galaxy. In this work, the value that we used was $\alpha_{nova}=0.0028$ and that allowed us to correctly reproduce the observed nova rate in the Galaxy, which is $20 \div 40$ events/yr (Della Valle & Izzo 2020). Indeed, our model prediction is $(Rate)_{Novae}=31$ number/yr. In particular, we define the rate of novae as:

$$(Rate)_{Novae}(t) = \alpha \int_{0.8 M_{\odot}}^{8 M_{\odot}} \psi(t - \tau_{m_2} - \Delta t) \varphi(m) dm, \quad (16)$$

with Δt being the delay time between the formation of the WD and the first nova outburst (the WD needs to cool down before the nova outburst can occur) and τ_{m_2} the lifetime of the secondary star that determines the start of the mass accretion onto the WD.

We had to consider that every nova system produces 10^4 nova outbursts, so if we want to compute the nova rate we need to multiply the nova formation rate by this number. In Figure 4, we show the rates of WDs and novae together as functions of time. In Table 2 we report the total rates and total numbers of WDs, novae and nova outbursts.

The number of nova systems and nova outbursts that occurred until the moment of the formation of the Solar System, in the solar vicinity, is computed as:

$$N_{Novae} = \int_0^{9.2 \text{ Gyr}} (Rate)_{Novae} dt = 1.18 \cdot 10^6, \quad (17)$$

that lead us to the following result for the number of nova outbursts:

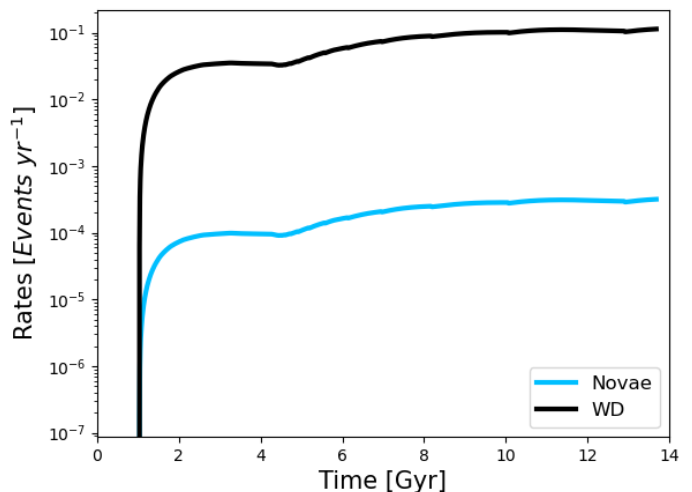


Fig. 4. Comparison of the rate of formation of nova systems and white dwarfs, in the solar vicinity.

$$N_{NO} = \int_0^{9.2 \text{ Gyr}} (Rate)_{NO} dt = 1.18 \cdot 10^{10}. \quad (18)$$

4.4. Neutron Stars

Neutron stars are among the densest objects known with an average density of around 10^{14} g/cm^3 . They are remnants of massive stars, but it is not clear the upper mass limit for the formation of a neutron star. In fact, if the stellar core is larger than the so-called Oppenheimer-Volkoff mass ($\sim 2 M_{\odot}$), then a black hole will form. The limiting initial stellar mass between the formation of a neutron star and a black hole is strongly dependent upon assumptions in stellar models, such as for example the rate of mass loss during the evolution of massive stars. In the model adopted here to compute the rate of neutron stars, we assumed that stars with masses from 9 to $50 M_{\odot}$ (Molero et al. 2023) leave a neutron star after their death. With this assumption we found that the rate of Neutron Stars is $(Rate)_{NS} \approx 2.93 \times 10^4$ number/Myr.

4.4.1. Merging Neutron Stars

Merging Neutron Stars (MNS) are important for what concerns the chemical evolution of galaxies, as they produce r-process elements. It was confirmed by the gravitational event GW170717 (Abbott et al. 2017) that the merging of neutron stars can produce a strong gravitational wave and that their contribution to the chemical composition of galaxies cannot be ignored. The rate of

Table 2. Comparison between observational data about nova outburst s (Della Valle & Izzo 2020) and model results relative to the rates of formation of WDs, nova systems and nova outburst rate. The legenda is like in Table 1. We note that the observed rates of formation of WDs and nova systems are not available, so only the theoretical values are shown. We can see that both values computed for nova outbursts are consistent with observational data.

	Observational Data (whole disc, present-day)	Rates (whole disc, present-day)	Numbers (solar vicinity, 9.2 Gyr of evolution)
Nova systems	–	0.0031 <i>events/yr</i>	1.18 <i>million</i>
Nova outbursts	25 – 30 <i>events/yr</i>	31 <i>events/yr</i>	11.8 <i>billion</i>
White dwarfs	–	1.11 <i>events/yr</i>	423 <i>million</i>

MNS and their number, is assumed to be proportional to the rate of formation of neutron stars (as proposed by Matteucci et al. 2014), namely:

$$(Rate)_{MNS} = \alpha_{NS} \cdot (Rate)_{NS}. \quad (19)$$

The constant α_{NS} is set to $\sim 10^{-3}$, chosen to correctly reproduce the observational rate of $83^{+209.1}_{-66.1}$ MNS/Myr (Kalogera et al. 2004) in the Milky Way. Finally, the total number of neutron stars and MNS that contributed to the chemical composition of the Solar System, in the solar vicinity, were obtained as the time integral of their rates, namely:

$$N_{NS} = \int_0^{9.2 \text{ Gyr}} (Rate)_{NS} dt = 23.15 \cdot 10^6, \quad (20)$$

and

$$N_{MNS} = \int_0^{9.2 \text{ Gyr}} (Rate)_{MNS} dt = 0.11 \cdot 10^6. \quad (21)$$

A plot with both neutron stars and MNS rates is provided in Figure 5. The total numbers can be found in Table 3.

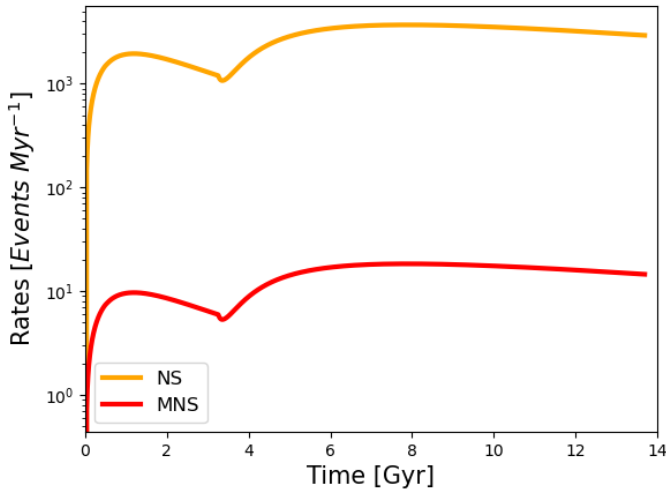


Fig. 5. Rates of neutron star (NS, yellow line) formation and merging neutron star (MNS, red line) predicted by our chemical evolution model for the solar vicinity.

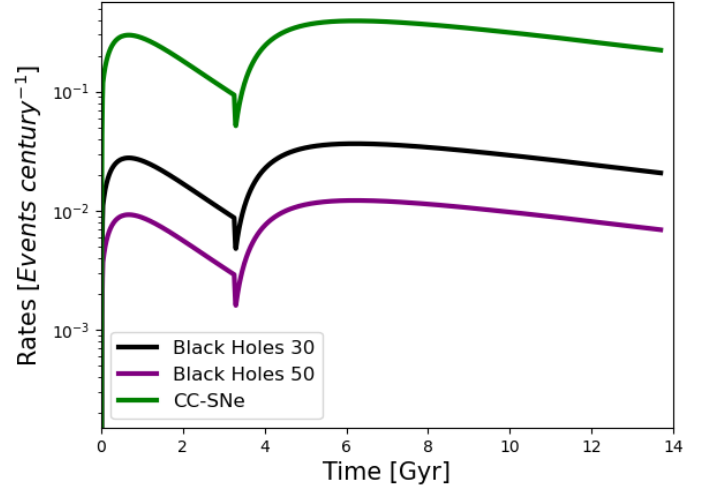


Fig. 6. Comparison between the rate of black holes that come from stars with masses $\geq 30 M_{\odot}$ (black line) and from stars with masses $\geq 50 M_{\odot}$ (purple line) with CC-SNe (green line), in the solar vicinity.

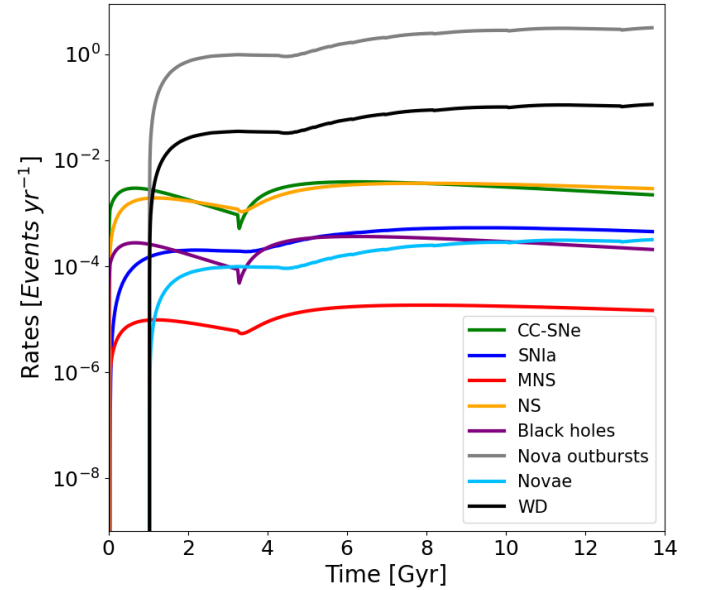


Fig. 7. Plot of the rates of all types stars in the solar vicinity, as discussed up until now. Notice that some types of stars, namely white dwarfs, novae and nova outbursts, started forming after $t \sim 1$ Gyr and not from the Big Bang.

Table 3. Comparison between observational data relative to the MNS rate in the Milky Way (Kalogera et al. 2004) and model results for neutron star formation and MNS rate. We can see that the computed value for the MNS rate is consistent with observational data and results by Molero et al. (2021). Notice that these values were obtained with $\alpha_{NS} = 0.005$

	observational Data (whole disc, present-day)	Rates (whole disc, present-day)	Numbers (solar vicinity, 9.2 Gyr of evolution)
Neutron Stars	–	29261 events/Myr	23.15 million
MNS	$83^{+209.1}_{-66.1}$ events/Myr	146 events/Myr	0.11 million

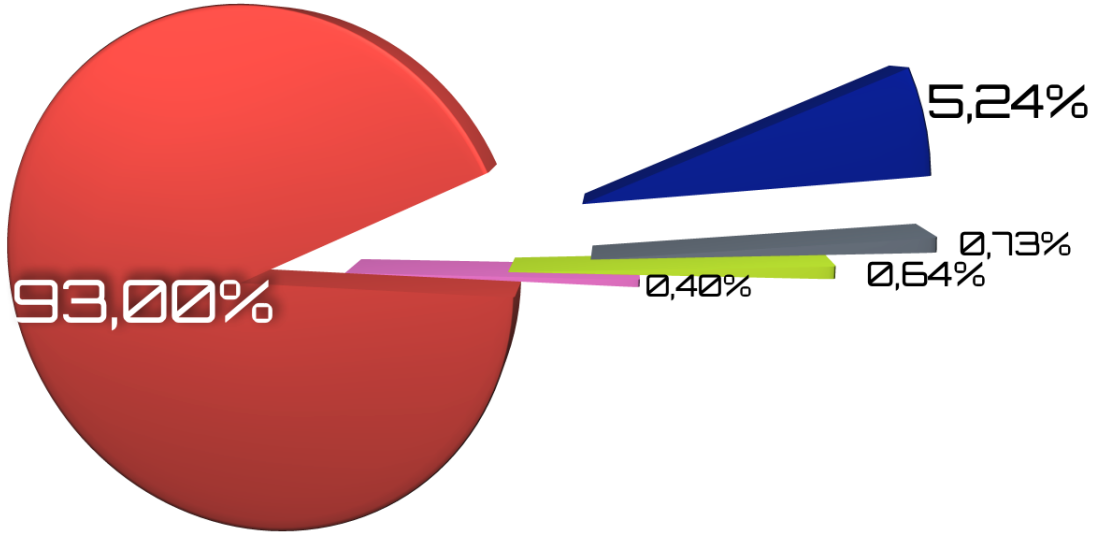


Fig. 8. Here we represent the percentages of all the stars that have contributed to the chemical composition of the Solar System, as analysed in this paper (see legenda).

Table 4. Comparison between different model results about the number of black holes with $M_{BH} \geq 30 M_{\odot}$ and $M_{BH} \geq 50 M_{\odot}$ as a percentage of massive stars.

Black holes	$M_{BH} \geq 30 M_{\odot}$	$M_{BH} \geq 50 M_{\odot}$
Percentage	9.14%	3.00%
Number	2.46 million	0.82 million

4.5. Black Holes

The last rate that we computed is the rate of birth of black holes originating from the massive stars that can leave a black hole after their death. The rate of formation of black holes is:

$$(Rate)_{BH}(t) = \int_{M_{BH}}^{100 M_{\odot}} \psi(t)\varphi(m) dm \quad (22)$$

In our model, we assumed two different values of M_{BH} (the limiting initial stellar mass for having a black hole as a remnant), namely $M_{BH}=30 M_{\odot}$ and $M_{BH}=50 M_{\odot}$. The total number

of black holes that formed until the formation of the Solar System is computed as:

$$N_{BH} = \int_0^{9.2 Gyr} (Rate)_{BH} dt. \quad (23)$$

The first choice, $M_{BH}=30 M_{\odot}$, led us to the result that roughly 9.14% of massive stars will leave a black hole, which means $N_{BH} \sim 2.46 \cdot 10^6$, while for $M_{BH}=50 M_{\odot}$ the number drops to 3.00%, that is $N_{BH} \sim 0.82 \cdot 10^6$.

In Figure 6, we provide a comparison between the rate of black holes under the assumptions of $M_{BH} \geq 30 M_{\odot}$ and $M_{BH} \geq 50 M_{\odot}$, as well as the rate of CC-SNe.

4.6. Comparison of all the rates

To have a complete vision of all types of stars that contributed to the formation of the Solar System and to its chemical evolution it is interesting to plot the different rates together, so that it is possible to better compare them.

In particular, in Figure 7, we report all the rates discussed up to now together for comparison. It is clear from the Figure

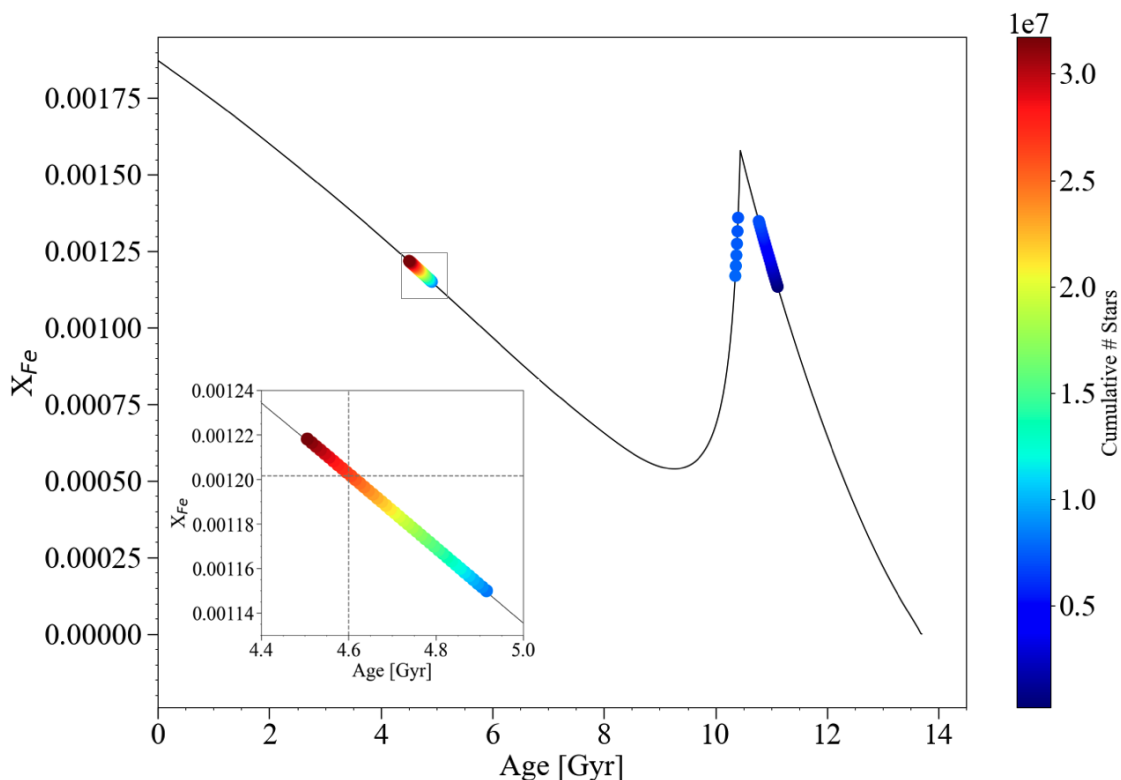


Fig. 9. Iron mass fraction X_{Fe} versus Galactic age, obtained with our chemical evolution model for the solar vicinity. With the colour-coded points, we highlight the cumulative number of stars sharing the same physical and chemical properties of our Sun formed from the beginning up to 4.6 ± 0.1 Gyr ago (see Section 5 for further details). In the inset plot we zoom-in the region with predicted Sun-like stars younger than 4.91 Gyr. The horizontal dashed line indicates the iron mass fraction predicted for our Sun born 4.6 Gyr ago (vertical dashed line).

that the nova outbursts, for the assumptions made, represent the largest number of events, but the material ejected during each burst is much less than what is produced by SNe and MNS. However, novae cannot be neglected in chemical evolution models since they can be responsible for the production of some important species. We underline that black holes ($M_{BH}=30 M_{\odot}$) are represented in this graph even if they do not contribute to the chemical enrichment, but they are related to very massive stars that can eject large amounts of metals before dying. Moreover, stars leaving black holes as remnants (Type Ib and Ic SNe) seem to be related to long GRBs, and the rate of formation of black holes can therefore trace the rate of these events (see Bissaldi et al. 2007).

In Figure 8, we show a stellar pie illustrating the different percentages of stellar contributors to the chemical composition of the Solar System. Clearly, the majority of stars ever born and dead from the beginning to the formation of the Solar System are belonging to the range of low and intermediate masses; these stars have mainly contributed to the production of He, some C, N and heavy s-process elements, while the massive stars, whose remnants are neutron stars and black holes, have produced the bulk of α -elements, in particular O which dominates the total solar metallicity Z . On the other hand, the bulk of Fe originated from Type Ia SNe. The novae can be important producers of CNO isotopes (see Romano 2022) and perhaps ${}^7\text{Li}$ (see Izzo et al. 2015; Cescutti & Molero 2019; Matteucci et al. 2021). Concerning r-process elements, the most reasonable assumption is that they have been produced in the range of massive stars both from merging neutron stars and, eventually, some peculiar type of CC-SNe (see Simonetti et al. 2019; Molero et al. 2023).

5. The number of stars similar to Sun born from the beginning up to the formation of the Solar System

In order to investigate a crucial aspect of the general argument of the evolution of the Galactic population of stars and their habitable planets, let us introduce the concept of the number of solar twins born before our Sun. Although it is known that also M stars ($0.08\text{-}0.45 M_{\odot}$) can host Earth-like planets and the numbers of these stars have been computed for the Milky Way (see Spitoni et al. 2017), here we focus on Solar-like stars as exoplanet hosts. Hence, we compute the number of stars in the range of mass $0.92\text{-}1.08 M_{\odot}$ born from the beginning up to 4.6 ± 0.1 Gyr ago and with solar Fe abundance compatible (within 1σ) with the value from Asplund et al. (2009) who reported 7.50 ± 0.04 dex. These stars represent all the possible Suns and, as a consequence, may indicate the number of possible planetary systems similar to ours ever existed in the solar neighbourhood. In those planetary systems there could be a planet like the Earth. This number is equal to $3.1732 \cdot 10^7$. Our Sun is the $2.6092 \cdot 10^7$ -th star of its kind, born in solar vicinity with a predicted Fe abundance of 7.48 dex, in excellent agreement with the observed one.

In Figure 9, we show the Fe abundance by mass as a function of the age, as predicted for the solar vicinity. The peak at early times corresponds to the formation of the thick disk, it follows a gap due to the strong decrease of the SFR and then an increase again up to the time of formation of the Solar System and beyond. Additionally, the figure shows the cumulative number of stars with the same mass and Fe abundance formed up to the appearance of our Sun. Notably, during the age interval from

11.12 Gyr to 10.36 Gyr, a total of 0.77377×10^7 solar-like stars were formed. Due to the strong chemical dilution from infalling gas with a pristine chemical composition associated with the thin disk phase, the Fe abundance remained sub-solar until 4.91 Gyr ago. In more recent times, i.e. Galactic ages between 4.91 and 4.50 Gyr, 2.39943×10^7 Suns were formed ($\sim 75.61\%$ of the total number).

We also computed the number of stars in the range of mass $0.92\text{--}1.08 M_{\odot}$ born 4.6 ± 0.1 Gyr ago in the solar vicinity, which is equal to $1.1325 \cdot 10^7$. In this case, the predicted Fe abundance values (expressed by number, i.e. $\log(\text{Fe}/\text{H})+12$) for our Sun-like stars range between 7.47 and 7.49 dex, hence in perfect agreement with the observed abundance of [Asplund et al. \(2009\)](#) (7.50 ± 0.04 dex). Our Sun is the $5.6856 \cdot 10^6$ -th star of its kind, born in solar vicinity with the associated Fe abundance of 7.48 dex.

6. Conclusions

In this work we have calculated the rates and the relative numbers of stars of different masses, which died either quiescently or in an explosive way as SNe, that contributed to the chemical composition of the Solar System (which formed about 4.6 Gyr ago) in the context of the two-infall model for the chemical evolution of the Milky Way.

Our results for each type of stars residing in the solar vicinity, can be summarised as follows:

- **Number of Type Ia supernovae:** 2.87 millions
- **Number of core-collapse supernovae:** 26.47 millions
- **Number of white dwarfs:** 423.88 millions
- **Number of nova systems:** 1.8 millions
- **Number of nova outbursts:** $1.8 \cdot 10^4$ millions
- **Number of neutron stars:** 23.5 millions
- **Number of merging neutron stars:** 0.11 millions
- **Number of black holes ($M \geq 30 M_{\odot}$):** 2.46 millions
- **Number of black holes ($M \geq 50 M_{\odot}$):** 0.82 millions

It is worth noting that all these numbers should be divided by 25 if one wants to restrict the solar vicinity area to a square centered in the Sun with a side of 2 kpc. Concerning the percentage of black holes that formed until the birth of the Solar System, in relation to the number of massive stars ($8 M_{\odot} \leq M \leq 100 M_{\odot}$), we found that only 3% of massive stars have the necessary characteristics to become black holes if we assume a limiting mass for the formation of black holes $\geq 50 M_{\odot}$, while the percentage increases to 9% if we accept stars with $M \geq 30 M_{\odot}$. We also obtained the total number of stars ever born and still alive at the time formation of the Sun and this number is $35.03 \cdot 10^8$.

Finally, the number of stars similar to the Sun born from the beginning up to 4.6 ± 0.1 Gyr ago in the metallicity range $12+\log(\text{Fe}/\text{H})=7.50 \pm 0.04$ dex is $3.1732 \cdot 10^7$, and in particular our Sun is the $2.6092 \cdot 10^7$ -th star of this kind, born in the solar vicinity.

Acknowledgement

F. Matteucci, M. Molero and A. Vasini thank I.N.A.F. for the 1.05.12.06.05 Theory Grant - Galactic archaeology with radioactive and stable nuclei. F. Matteucci also thanks Ken Crowell for stimulating the computation of the total number of novae, thus giving the idea for the present paper. This research was supported by the Munich Institute for Astro-, Particle and Bio-Physics (MIAPbP) which is funded by the Deutsche Forschungsgemeinschaft (DFG, German Research Foundation) under Germany's Excellence Strategy – EXC-2094 – 390783311. F. Matteucci thanks also support from Project PRIN MUR 2022 (code

2022ARWP9C) "Early Formation and Evolution of Bulge and Halo (EFEBHO)" (PI: M. Marconi), funded by the European Union – Next Generation EU. E. Spitoni thanks I.N.A.F. for the 1.05.23.01.09 Large Grant - Beyond metallicity: Exploiting the full Potential of CHEMICAL elements (EPOCH) (ref. Laura Magrini). This work was supported by the Deutsche Forschungsgemeinschaft (DFG, German Research Foundation) – Project-ID 279384907 – SFB 1245, the State of Hessen within the Research Cluster ELEMENTS (Project ID 500/10.006).

References

- Abbott, B. P., Abbott, R., Abbott, T. D., et al. 2017, *Phys. Rev. Lett.*, 119, 161101
- Asplund, M., Grevesse, N., Sauval, A. J., & Scott, P. 2009, *ARA&A*, 47, 481
- Bissaldi, E., Calura, F., Matteucci, F., Longo, F., & Barbiellini, G. 2007, *A&A*, 471, 585
- Bouvier, A. & Wadhwa, M. 2010, *Nature Geoscience*, 3, 637
- Cappellaro, E. & Turatto, M. 1997, in *NATO Advanced Science Institutes (ASI) Series C*, Vol. 486, NATO Advanced Science Institutes (ASI) Series C, ed. P. Ruiz-Lapuente, R. Canal, & J. Isern, 77
- Cescutti, G. & Molaro, P. 2019, *MNRAS*, 482, 4372
- Chiappini, C., Matteucci, F., & Gratton, R. 1997, *ApJ*, 477, 765
- Chiappini, C., Matteucci, F., & Romano, D. 2001, *ApJ*, 554, 1044
- Della Valle, M. & Izzo, L. 2020, *A&A Rev.*, 28, 3
- Ekström, S., Meynet, G., Chiappini, C., Hirschi, R., & Maeder, A. 2008, *A&A*, 489, 685
- Fuhrmann, K. 1998, *A&A*, 338, 161
- Gratton, R., Carretta, E., Matteucci, F., & Sneden, C. 1996, in *Astronomical Society of the Pacific Conference Series*, Vol. 92, *Formation of the Galactic Halo...Inside and Out*, ed. H. L. Morrison & A. Sarajedini, 307
- Greggio, L. 2005, *A&A*, 441, 1055
- Grisoni, V., Spitoni, E., & Matteucci, F. 2018, *MNRAS*, 481, 2570
- Grisoni, V., Spitoni, E., Matteucci, F., et al. 2017, *MNRAS*, 472, 3637
- Hayden, M. R., Bovy, J., Holtzman, J. A., et al. 2015, *ApJ*, 808, 132
- Hayden, M. R., Holtzman, J. A., Bovy, J., et al. 2014, *AJ*, 147, 116
- Hirschi, R. 2005, in *From Lithium to Uranium: Elemental Tracers of Early Cosmic Evolution*, ed. V. Hill, P. Francois, & F. Primas, Vol. 228, 331–332
- Hirschi, R. 2007, *A&A*, 461, 571
- Iwamoto, K., Brachwitz, F., Nomoto, K., et al. 1999, *ApJS*, 125, 439
- Izzo, L., Della Valle, M., Mason, E., et al. 2015, *ApJ*, 808, L14
- Kalogera, V., Kim, C., Lorimer, D. R., et al. 2004, *ApJ*, 614, L137
- Karakas, A. I. 2010, *MNRAS*, 403, 1413
- Kawata, D. & Chiappini, C. 2016, *Astronomische Nachrichten*, 337, 976
- Kennicutt, Jr., R. C. 1998, *ApJ*, 498, 541
- Kobayashi, C., Umeda, H., Nomoto, K., Tominaga, N., & Ohkubo, T. 2006, *ApJ*, 653, 1145
- Kroupa, P., Tout, C. A., & Gilmore, G. 1993, *MNRAS*, 262, 545
- Li, W., Chornock, R., Leaman, J., et al. 2011, *MNRAS*, 412, 1473
- Matteucci, F. 2012, *Chemical Evolution of Galaxies*
- Matteucci, F. 2021, *A&A Rev.*, 29, 5
- Matteucci, F. & Francois, P. 1989, *MNRAS*, 239, 885
- Matteucci, F. & Greggio, L. 1986, *A&A*, 154, 279
- Matteucci, F., Molero, M., Aguado, D. S., & Romano, D. 2021, *MNRAS*, 505, 200
- Matteucci, F., Romano, D., Arcones, A., Korobkin, O., & Rosswog, S. 2014, *MNRAS*, 438, 2177
- Melioli, C., Brighenti, F., D'Ercole, A., & de Gouveia Dal Pino, E. M. 2009, *MNRAS*, 399, 1089
- Meynet, G. & Maeder, A. 2002, *A&A*, 390, 561
- Micali, A., Matteucci, F., & Romano, D. 2013, *MNRAS*, 436, 1648
- Mikolaitis, Š., de Laverny, P., Recio-Blanco, A., et al. 2017, *A&A*, 600, A22
- Molero, M., Magrini, L., Matteucci, F., et al. 2023, *MNRAS*, 523, 2974
- Molero, M., Simonetti, P., Matteucci, F., & della Valle, M. 2021, *MNRAS*, 500, 1071
- Paczynski, B. 1998, *ApJ*, 494, L45
- Palla, M., Matteucci, F., Spitoni, E., Vincenzo, F., & Grisoni, V. 2020, *MNRAS*, 498, 1710
- Prantzos, N., Abia, C., Limongi, M., Chieffi, A., & Cristallo, S. 2018, *MNRAS*, 476, 3432
- Recio-Blanco, A., de Laverny, P., Kordopatis, G., et al. 2014, *A&A*, 567, A5
- Recio-Blanco, A., de Laverny, P., Palicio, P. A., et al. 2023, *A&A*, 674, A29
- Romano, D. 2022, *A&A Rev.*, 30, 7
- Romano, D., Chiappini, C., Matteucci, F., & Tosi, M. 2005, *A&A*, 430, 491
- Romano, D., Karakas, A. I., Tosi, M., & Matteucci, F. 2010, *A&A*, 522, A32
- Romano, D., Matteucci, F., Salucci, P., & Chiappini, C. 2000, *ApJ*, 539, 235
- Romano, D., Matteucci, F., Zhang, Z.-Y., Ivison, R. J., & Ventura, P. 2019, *MNRAS*, 490, 2838

- Schmidt, M. 1959, *ApJ*, 129, 243
- Simonetti, P., Matteucci, F., Greggio, L., & Cescutti, G. 2019, *MNRAS*, 486, 2896
- Spitoni, E., Giovannini, L., & Matteucci, F. 2017, *A&A*, 605, A38
- Spitoni, E., Matteucci, F., Gratton, R., et al. 2024, arXiv e-prints, arXiv:2405.11025
- Spitoni, E., Silva Aguirre, V., Matteucci, F., Calura, F., & Grisoni, V. 2019, *A&A*, 623, A60
- Spitoni, E., Verma, K., Silva Aguirre, V., & Calura, F. 2020, *A&A*, 635, A58
- Spitoni, E., Verma, K., Silva Aguirre, V., et al. 2021, *A&A*, 647, A73
- Tinsley, B. M. 1979, *ApJ*, 229, 1046
- Yoon, S. C., Woosley, S. E., & Langer, N. 2010, *ApJ*, 725, 940